

**Invited paper: "Advances in Materials Characterization", University Series
on Ceramic Science, Alfred University, Alfred N. Y., August 15-18, 1982.**

**EM STUDY OF THE STRUCTURE AND COMPOSITION OF GRAIN
BOUNDARIES IN $(\text{Mn},\text{Zn})\text{Fe}_2\text{O}_4$**

I-Nan Lin, R. K. Mishra and G. Thomas

Materials and Molecular Research Division

Lawrence Berkeley Laboratory

University of California

Berkeley, CA 94720

DISCLAIMER

This report was prepared in the course of work sponsored by an agency of the United States Government. Neither the United States Government nor any agency thereof, nor any of their employees, makes any warranty, express or implied, or assumes any legal liability or responsibility for the accuracy, completeness, or usefulness of any information, apparatus, product, or process disclosed, or represents that its use would not infringe privately owned rights. Reference herein to any specific commercial product, process, or service by trade name, trademark, manufacturer, or otherwise does not necessarily constitute or imply its endorsement, recommendation, or favoring by the United States Government or any agency thereof. The views and opinions of authors expressed herein do not necessarily state or reflect those of the United States Government or any agency thereof.

680

ABSTRACT

Electron diffraction and microscopy studies supplemented by electron spectroscopic techniques such as Auger electron spectroscopy and energy dispersive x-ray spectroscopy were used to characterize the nature of grain boundary segregation in commercial grade $(\text{Mn}, \text{Zn})\text{Fe}_2\text{O}_4$ samples containing small quantities of CaO . Chemical analyses by AES and EDAX show an enrichment of Ca near the grain boundary region. Convergent beam electron diffraction experiments show that the crystal symmetry of the spinel structure is distorted in the vicinity of the grain boundary. In-situ heating experiments in HVEM show the existence of a disordered phase at the sintering temperature. Lorentz microscopy in TEM shows the interaction of magnetic domain wall motion with grain boundaries. These chemical and structural features are correlated with electrical resistivity and magnetic permeability of the ferrites.

INTRODUCTION

The presence of any second phases at grain boundaries in polycrystalline ceramics has been of great interest for their effects on the mechanical or electronic properties. In the case of high temperature structural ceramics, such as Si_3N_4 , the amorphous boundary phase is responsible for low temperature creep.¹ In the case of electronic materials, such as PZT, ZnO varistors and soft ferrites, the presence of a thin grain boundary layer drastically affects the electrical and magnetic properties.² The formation of the second phase at grain boundaries in ceramic materials is very common and a complete characterisation of these second phases can be

done only by modern techniques, such as transmission electron microscopy (TEM), analytical electron microscopy (AEM) and Auger electron spectroscopy (AES). In the present work, the physical and chemical characterization of an amorphous grain boundary phase in $(\text{Mn},\text{Zn})\text{Fe}_2\text{O}_4$ using the above-mentioned techniques and the effects of this phase on the electrical and magnetic properties of the material will be discussed.

The $(\text{Mn},\text{Zn})\text{Fe}_2\text{O}_4$ is a soft ferrite with high initial permeability (μ_i). Small amounts of CaO are added in commercial $(\text{MnZn})\text{Fe}_2\text{O}_4$ to increase the electrical resistivity through the formation of an insulating layer along the grain boundaries.³ The existence of a thin intergranular amorphous phase has been observed by Mishra et al.⁴ using lattice fringe image microscopy⁵ and also by Lin et al.⁶ using high resolution dark field microscopy.⁷ It has been shown that the grain boundary phase is enriched in Ca. A complete characterization of the grain boundary and its effects upon the magnetic properties and sintering mechanism has not been ascertained, but will be discussed in this work.

EXPERIMENTAL

Sintered specimens of MnZn ferrite with the nominal composition of $\text{MnO}:\text{ZnO}:\text{Fe}_2\text{O}_3 = 26.9:19.8:53.3$ (mole %) and with the major additive of CaO (2543 ppm) were supplied by TDK Electronics Co. of Japan. A 1mm x 5mm x 10mm slice of sintered material was fractured in-situ in a Physical Electronics 590 scanning Auger electron microscopy^{8,9} and the chemical composition was determined from Auger electron spectra. Electron transparent thin foils were prepared from the bulk sample by an ion milling

technique. The magnetic domain wall structure and its interaction with grain boundaries were studied in a Philips EM301 microscope using Lorentz microscopy (LM).^{10,11} The symmetry of the crystal structure was studied in a Philips EM400 microscope using convergent beam electron diffraction (CBD).¹² The behavior of Ca-doped grain boundaries at high temperature was studied by heating a thin foil in the hot stage of the Osaka University 3MeV high voltage electron microscope (HVEM) to a temperature of 1400°C.

RESULTS

A typical AES spectrum from a fractured surface of MnZn ferrite (Fig. 1b) clearly shows the existence of Ca. Careful experiments show that the Ca signal comes from those regions of the surface that are intergranular fracture. The Ca-signal completely disappears after the fractured surface is sputtered in-situ by argon ions for ~ six minutes. Since the escape depth of the Auger electrons is less than 20 \AA and the sputtering rate is only about 10 $\text{\AA}/\text{min.}$, the thickness of the Ca containing phase is about 60 \AA . Besides the Ca signal indicated in Fig. 1b, the spectra from intergranular fracture surfaces also have Fe and Mn signals. This implies that the Ca-containing phase is not a pure CaO phase as proposed by other authors.^{3,13,14} Although the chemical composition is very difficult to determine quantitatively, it can be concluded that the Ca-containing phase is an intermediate compound of CaO and MnZn ferrite. The existence of the intermediate compound has also been confirmed by Lin et al. by SEM hot stage experiments.⁶ The Ca signal is observed only when the electron probe, 500 \AA in diameter, is placed at intergranular fracture surfaces. No

Ca peak is observed when the electron probe is placed at transgranular fracture surfaces (Fig. 1a). This indicates that the Ca-containing layer only forms a thin layer along grain boundaries. This grain boundary phase exists as an amorphous phase,^{4,6} as has been shown elsewhere. It occurs due to the difficulty of crystallization of thin layers of liquid trapped between grains.^{15,16}

The interaction of grain boundaries and magnetic domain walls is shown in Fig. 2. When the electron microscope is operated in the Lorentz mode, the images of the magnetic domain walls appear as either bright or dark fringes, depending on the relative orientation of the magnetization vector in the two adjacent magnetic domains. The domain walls reverse the contrast between overfocus and underfocus. The technique can be used to differentiate between the domain walls and other linear defects such as grain boundaries and dislocations.

The domain configurations in Fig. 2 show the sequence of domain wall positions with increasing applied magnetic field. The domain walls which appear as bright fringes in the overfocused situation, labelled O, are plotted as solid lines and the ones which appear as bright fringes in the underfocused situation, labelled U, are plotted as dashed lines in the central sketch. The grain boundaries, on the other hand, are plotted as dotted lines. As the applied magnetic field increases, the domains B and C will grow; the solid line will move to the right and the dashed line will move to the left. The domain A, which is bounded partly by grain boundaries, is not able to change as the domain wall 1-1 is unable to move toward the grain boundary under a moderate applied magnetic field (Figs. 2a and 2b). Only after the applied magnetic field is raised appreciably will the domain A change its magnetization vector, and the domain wall 1-1 will

jump to the grain boundary abruptly. This domain wall will not be able to move across the grain boundary even when the magnetic field is increased further (Fig. 2c).

While the Ca-segregated grain boundaries will stop the domain wall motion completely, it has been observed that the domain wall can move across the grain boundaries when they are free of segregation¹⁷. Lorentz microscopy techniques in TEM thus provide a promising approach for in-situ study of the interaction of the microstructure with domain wall motion, an experiment that is not possible by other techniques.

The nature of the grain boundary region was further examined by convergent beam electron diffraction (CED). In this technique, a convergent electron beam is used to form the diffraction pattern instead of a defocussed parallel beam. The CBD pattern typically consists of disks, each of which corresponds to a Bragg diffraction spot in conventional diffraction mode. The sharp line pattern in the central disk, called high order Laue zone (HOLZ) lines, and the intensity distribution in the surrounding disks are sensitive to the changes in both crystal symmetry and lattice parameter.¹³

The CBD patterns of the Spinel ferrite $(\text{Mn}, \text{Zn})\text{Fe}_2\text{O}_4$ with the electron beam incident along the [001] zone axis are shown in Fig. 3. When the electron probe, 0.2μ in diameter, is put in the interior of the grain, both the HOLZ lines and the intensity distribution show 4mm crystallographic symmetry for $\text{Fd}3\text{m}$ symmetry of the spinel structure (Fig. 3a). If the probe is placed in the region near grain boundaries, however, the CBD pattern no longer possesses such a high symmetry; the HOLZ lines have only 2mm symmetry and the intensity distribution is only of m symmetry

(Fig. 3b). The lowering of the crystallographic symmetry in the region near the grain boundary is ascribed to the dissolution of a small amount of Ca ions which are much larger than the other cations in $(\text{Mn}, \text{Zn})\text{Fe}_2\text{O}_4$.

The segregation of Ca at grain boundaries will affect the sintering mechanism of $(\text{Mn}, \text{Zn})\text{Fe}_2\text{O}_4$. In order to study the behavior of the Ca-segregated grain boundaries at the sintering temperature, a thin foil was heated in-situ in a hot stage using a high voltage electron microscope (HVEM). The results are shown in Fig. 4.

For temperatures below 1300°C, there is no noticeable reaction observed. However, when the temperature is raised to 1400°C, there are two important reactions observed near the grain boundaries: i) The image of grain boundaries changes from a sharp line (or fringes) to a diffuse line. The existence of a disordered phase at the grain boundaries at 1400°C is inferred from this observation. (ii) The positions of the three grain junctions are shifted due to grain boundary migration. The migration is more prominent in the junctions where the angle between grain boundaries originally deviated considerably from 120°C (e.g. junction a, b in Fig. 4).

DISCUSSION

The addition of small amounts of Ca is known to lead to the formation of a secondary phase along grain boundaries. It is concluded from the AES analysis that this grain boundary phase is an intermediate compound of CaO and MnZn-ferrite, and previous studies suggest that it exists in an amorphous form. In addition, the region near the grain boundaries must possess higher magnetic anisotropic energy and magneto-striction energy such that the

magnetization vectors can change the directions only under higher applied magnetic fields, as observed in Lorentz microscopy experiments. The increase in the magnetic energy of this region is ascribed to the lowering of crystal symmetry or localized strain, as confirmed by CBD technique. The effect of Ca-addition on the magnetic properties is to modify the grain boundary structure and its interaction with magnetic domain walls.

In the HVEM experiments the tendency of the grain boundaries to make equal angles with each other implies that the grain boundary surface energy is isotropic at high temperatures. This also supports the existence of either a disordered phase or a liquid phase at the grain boundaries, as the solid-liquid interfacial energy is known to be less anisotropic than the solid-solid interfacial energy. Furthermore, the existence of a eutectic liquid between CaO and the CaO-ferrite intermediate compound has been observed by in-situ heating of this material in SEM.⁶ In summary, these results, namely the existence of eutectic liquid, diffuse grain boundary image and grain boundary migration, strongly imply that the addition of CaO leads to the formation of a liquid phase at sintering temperatures and such a phase remains as an intergranular phase after the sample has been cooled.

CONCLUSION

The grain boundary phase in MnZn-ferrite plays an important role in determining the electrical and magnetic properties. Addition of a small amount of Ca in these materials increases the electrical resistivity, as well as the coercivity of the materials, but lowers the initial permeability. All these effects can be ascribed to the segregation of Ca at grain boundaries in the form of an amorphous intermediate phase.

The interaction of the grain boundaries with magnetic domain wall motion studied by Lorentz microscopy and CBD technique in TEM provides an understanding of the effect of microstructure on the magnetic properties. In-situ heating in HVEM results in an understanding of the behavior of grain boundary phase at sintering temperatures. Finally, these TEM techniques in conjunction with analytical techniques such as AES and x-ray analysis in STEM, provide a promising approach towards understanding the effect of grain boundaries upon the behavior of ceramic materials.

ACKNOWLEDGEMENTS

This work was supported by the Director, Office of Energy Research, Office of Basic Energy Sciences, Materials Sciences Division of the U. S. Department of Energy under Contract No. DE-AC03-76SF00098. Special thanks from Lin to INER (R.O.C.) for financial assistance. Special thanks are due to TDK Electronics Co. of Japan for supplying the MnZn ferrite samples and Professor H. Fujita for arranging the hot stage HVEM experiments. Drs. H. Mori and M. Komatsu performed the in-situ HVEM experiments on the 3MeV microscope at Osaka University.

REFERENCES

1. R. C. Bradt and R. E. Tressler, "Deformation of Ceramic Materials", Plenum, New York (1975).
2. L. M. Levinson, "Grain Boundary Phenomena in Electronic Ceramics; Advances in Ceramics, Vol. 1", The American Ceramic Society, Inc., Columbus, Ohio (1980).
3. The Akashi, Tran. Japan. Inst. Metals 2:171 (1961).
4. R. K. Mishra, E. K. Goo and G. Thomas, Amorphous Grain Boundary Phase in Ferrimagnetic $(\text{Mn},\text{Zn})\text{Fe}_2\text{O}_4$ and Ferroelectric PZT Ceramics in: "Surface and Interface in Ceramic and Ceramic-Metal Systems", J. Pask and A. G. Evans, eds., Plenum Press, New York (1981).
5. J. Spence, "Experimental High-Resolution Electron Microscopy", Clarendon Press, Oxford (1981).
6. I. N. Lin, R. K. Mishra and G. Thomas, "Ca-segregation in $(\text{Mn},\text{Zn})\text{Fe}_2\text{O}_4$ ", in press, IEEE Magnetics, 1982.
7. O. L. Krivanek, T. M. Shaw and G. Thomas, J. Appl. Physics 50:4423 (1979).
8. L. E. Davis *et al.*, "Handbook of Auger Electron Spectroscopy, 2nd ed.", Physical Electronics Industries, Inc. (1972).
9. P. M. Hall and J. M. Morabito, Compositional Depth Profiling by Auger Electron Spectroscopy, CRC Critical Review in Solid State and Materials Sciences, 53 (1978).
10. G. Thomas and M. J. Goringe, "Transmission Electron Microscopy of Materials", John Wiley and Sons, N. Y. (1979).
11. P. B. Hirsch *et al.*, "Electron Microscopy of Thin Crystals", Butterworths, London 388, (1971).

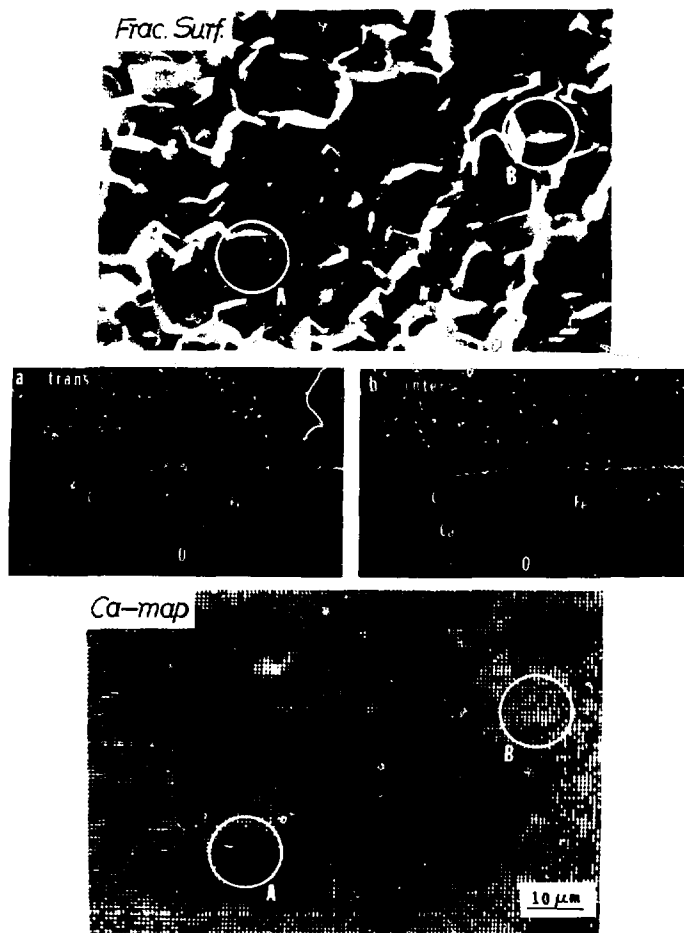
12. J. W. Steeds, Convergent Beam Electron Diffraction, Ch. 15 in: "Introduction to Analytical Electron Microscopy", J. J. Hren, J. I. Goldstein and D. C. Joy, eds., Plenum, New York (1979).
13. M. Paulus, Properties of Grain Boundaries in Spinel Ferrites, Ch. 3 in: "Materials Science Research, vol. 3" (1966).
14. P. F. Bongers, et al., Defects, Grain Boundary Segregation and Second Phases of Ferrites in Relation to Magnetic Properties, p. 265 in: "Ferrites: Proceedings of the ICF 3", H. Watanabe, S. Iida and M. Sugimoto, eds. (1980).
15. E. K. W. Goo, R. K. Mishra and G. Thomas, Transmission Electron Microscopy of $\text{Pb}(\text{Zr}_{0.52}\text{Ti}_{0.48})\text{O}_3$, J. Amer. Ceramic Soc. 64:517 (1981).
16. R. Raj, Morphology and Stability of the Glass Phase in Glass-Ceramic Systems, J. Amer. Ceramic Soc. 64:245 (1981).
17. I. N. Lin, Microstructure and Magnetic Domain Wall Motion, P324 in: "Proceedings of EMSA", Claitors Publishing House, New Orleans (1981).

Fig. 1. Auger electron spectrum of in-situ fracture surface: (a) transgranular and (b) intergranular fracture surface. The Ca signal is observed only at intergranular fracture surface.

Fig. 2. Interaction of grain boundaries with magnetic domain wall motion: domain configurations under a situation where a (a) zero, (b) moderate and (c) high magnetic field is applied. (i) the domains B and C grow as applied magnetic field is increasing; (ii) domain A will not grow under moderate applied magnetic field and it changes its magnetization abruptly under higher applied magnetic field.

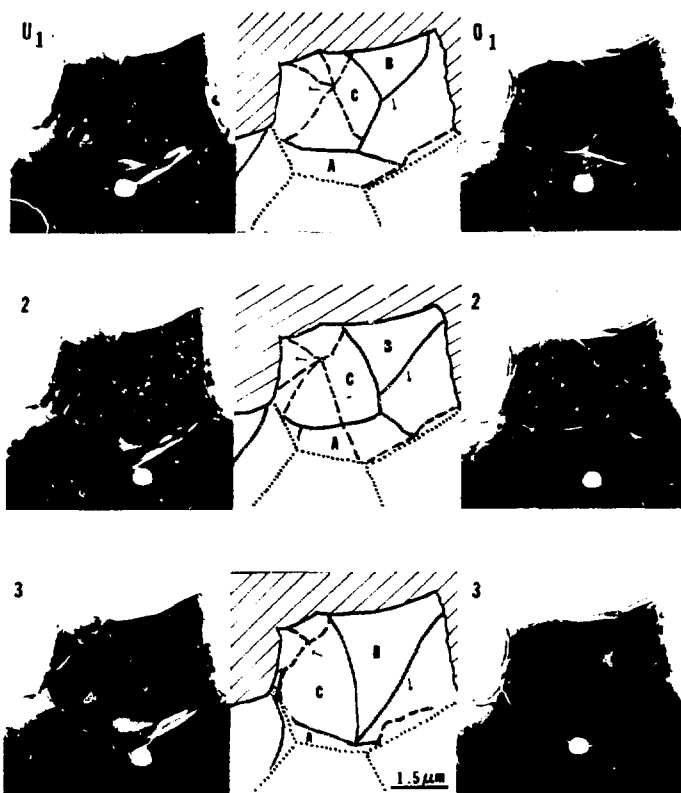
Fig. 3. CBD patterns of $(\text{Mn},\text{Zn})\text{Fe}_2\text{O}_4$ with electron beams incident along [001] zone axis and electron probe placed at (a) interior of the grain and (b) region near grain boundary respectively. The symmetry of the Holz lines in the central disk and the intensity distribution of the surrounding disks have lower symmetry in the region near grain boundaries.

Fig. 4. The grain boundary structure of $(\text{Mn},\text{Zn})\text{Fe}_2\text{O}_4$ at (a) 1300°C and (b) 1400°C respectively. (i) the grain boundary images become diffuse at higher temperature, (ii) grain boundary migration occurs at 3-grain junctions a and b.



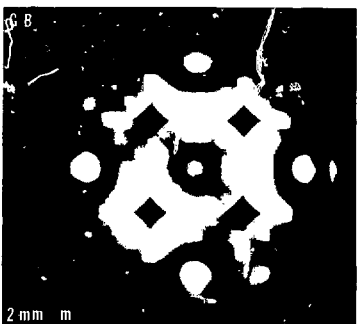
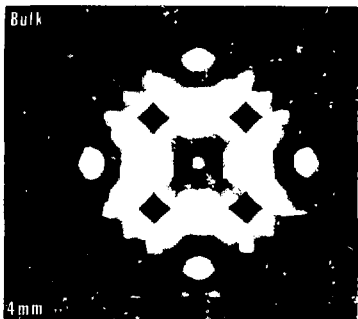
XBB 817-7041

Fig. 1



XBB 800-11965

Fig. 2



XBB 817-7040

Fig. 3



XBB 826-5218

Fig. 4